



The Use of UAVs (Unmanned Aerial Vehicles) in Agriculture



Contents

1. The Use of UAVs (Unmanned Aerial Vehicles) in Agriculture.....	4
2. CONCEPTUAL DESIGN OF UAV	8
2.1 Wing Configurations.....	8
2.2 Motor Placement.....	10
2.3 Tail	10
2.4 Body.....	10
2.5 Weight Estimation.....	11
2.6 Airfoil Selection	12
3. PRELIMINARY DESIGN	13
3.1 Methodology.....	13
3.2 Design-Sizing Trades	13
3.3 Aerodynamic Design.....	14
3.4 Fuselage	14
3.5 Wing Sizing.....	14
3.6 Understanding Slung Load.....	14
3.7 Stability and CFD Analysis.....	15
4. Estimations.....	18
4.1 Wing Area and Wing Load.....	18
4.2 Stall Speed Calculation	18
4.3 Bank Angle Calculation	18
4.4 Angle of Attack Calculation.....	19
4.5 Thrust Available Calculations	19
4.6 Maximum Cruise Speed.....	19
5. Power Consumption.....	20
5.1 Propulsion	20
5.2 Control Units.....	20
6. DETAILED DESIGN	21
6.1 Dimensions	21
6.2 3D Drawing Package	22
6.3 Weight and Balance.....	23
6.4 Body.....	24
6.5 Wing and Other Aerodynamic Surfaces.....	24

6.6 Structural Frame.....	24
6.7 Tail	24
6.8 Landing Gear	24
6.9 Release System	24
6.10 Anticipating Effects of the Slung Load.....	25
7. Avionics.....	25
7.2 Component Selection	25
7.3 Microcontroller	26
7.3.1 Option 1: Raspberry Pi 4 8GB	26
7.3.2 Option 2: Jetson Nano 4GB	26
7.4 Flight Controller.....	27
7.4.1 Option 1: Pixhawk Cube Orange	27
7.4.2 Option 2: Pixhawk 2.4.8	27
7.5 Battery.....	28
7.6 Electric Motors.....	29
7.7 Electronic Speed Controller.....	29
7.8 Servo Motors.....	30
7.9 Telemetry	30
7.10 Power and Propulsion System.....	31
8. Computer Vision and Target Detection System	32
8.1 First: Potential Target Detection.....	32
8.2 Second: Scanning Process	32
8.3 Third: Coordinate Transform	32
9. Control System and Units.....	33
9.1 Flight Controller	34
9.2 Companion Computer.....	34
9.3 Ground Station	35
10. Communication System	35
10.1 Pixhawk - Raspberry Pi 4.....	35
10.2 Ground Control Station and Communication.....	36

1. The Use of UAVs (Unmanned Aerial Vehicles) in Agriculture

Agriculture, although an essential sector, is a mandatory and strategic activity for the continuity of life. Due to the rapid increase in the world population and urbanization, agricultural areas are decreasing, leading to a reduction in natural resources such as agricultural land and water per capita (Özgüven and Közkurt, 2021). The primary goal of agricultural production is to ensure economic, sustainable, and productive management in both plant and animal production. To achieve this goal, various technologies are employed in agriculture to facilitate agricultural processes and develop alternative solutions for problems that require resolution or improvement (Özgüven, 2018). The agricultural sector is adversely affected by economic, social, structural, and climatic issues.

Some of these issues include global market fluctuations, economic crises, droughts, tornadoes, and floods resulting from climate change, diseases, the emergence of alternative uses for agricultural products such as biofuels, non-purpose use of agricultural land for mining activities, depletion of natural resources like water, and the increase in the elderly population in villages due to the migration of the younger population to urban areas. Therefore, the use of technology and genetic methods in agricultural production has become essential to increase productivity (Özgüven, 2020; Özgüven et al., 2020).

Improving productivity and product quality in agricultural production depends on closely monitoring the development process of plants and timely implementation of necessary practices. Drones with a simple technical structure and easy usability, equipped with sensors and cameras, capture high-resolution photos, and create 3D maps, providing farmers with planning opportunities in agricultural activities (Tan et al., 2015). Thus, current data related to agricultural activities can be collected, and efficiency in production can be achieved. Table 1 summarizes the advantages and disadvantages of using drones in agriculture.

Advantages	Disadvantages
Land data can be collected more quickly and easily.	Not suitable for irrigation.
In field research, the time spent is reduced by using UAVs instead of human labor.	Different countries have their own restrictive frameworks (legal uncertainties) regarding the use of drones in agriculture.
It enables the acquisition of high spatial resolution images of plants due to its ability to fly at low altitudes.	It cannot perform tasks on the same scale as traditional farming machinery.
The costs of fuel consumption for agricultural vehicles and the associated environmental damages are reduced.	Its usage is limited in adverse weather conditions.
Savings are achieved in both pesticide usage and energy consumption.	It involves issues such as data security (hacking, electromagnetic interference, signal loss) and concerns about privacy and confidentiality breaches.
Injuries that may occur due to the use of human labor are minimized.	The most significant problem is the inadequacy of battery life.

Table 1

Plant water requirements are mostly dependent on meteorological data such as rainfall and temperature, but they also vary from one plant species to another. For example, the water consumption of corn plants varies depending on the cultivated region and growth stages. Generally, it is around 550-600 mm on average. This value corresponds to 550-600 tons of water for irrigating one hectare of corn, and assuming irrigation is done 10 times during the growing season, the amount of water to be applied in each irrigation is

approximately 55-60 tons per hectare. Therefore, it does not seem feasible to achieve such irrigation amounts even with a drone on one hectare.

Another important aspect to be considered is delivering irrigation water to the root zone of the plant. Considering the height of the drone above the ground and environmental factors such as wind, it does not seem possible to perform this application with a drone. Additionally, irrigating with a drone may increase the moisture on plant leaves, potentially leading to the development of fungal and bacterial diseases.

In agriculture, the use of drones has been explored in various areas such as disease and pest detection, pesticide and fertilizer applications, weed detection, yield estimation, identification of plant stresses, monitoring crop development, plant species differentiation, seed planting, determination of phenological characteristics, water management practices, and herd management. Table 2 summarizes some agricultural studies conducted with drones by researchers.

Examples of UAV Applications in Agriculture	
Disease Detection	Altas ve ark., 2018; Su ve ark., 2018; Kitpo ve Inoue, 2018; Altaş ve ark., 2019; Kerkech ve ark., 2020; Syifa ve ark., 2020
Fertilizer Applications	Meivel ve ark., 2016; Yallappa ve ark., 2017; Garre ve ark., 2018; Babu ve ark., 2020; Chen ve ark., 2021
Monitoring Crop Development and Classification of Plants	Buters ve ark., 2019; Ore ve ark., 2020; D’Odorico ve ark., 2020; Maimaitijiang ve ark., 2020; Neumann ve ark., 2020; Matsuura ve ark., 2020; Fawcett ve ark., 2020
Detection of Weeds	Gašparović ve ark., 2020; Parra ve ark., 2020; Skacev ve ark., 2020; Mattivi ve ark., 2021
Yield Prediction	Reza ve ark., 2019; Stavrakoudis ve ark., 2019; Apolo-Apolo ve ark., 2020; Tao ve ark., 2020
Water Management Practices	Gago ve ark., 2015; Zhang ve ark., 2019; Dantas ve ark., 2020; Jin ve ark., 2021

Table 2

Plant Disease Detection

Altaş et al. (2018) conducted a study in which images taken from a sugar beet field using drones were processed with developed image processing algorithms to determine the presence of leaf spot disease (*Cercospora beticola* Sacc.) and the severity of the disease if present. For this purpose, 12 images showing different stages of disease development were captured at heights between 30-60 cm using a drone at various times and under different natural lighting conditions. These images were processed using the image processing toolbox of the MATLAB program. When the results of the study conducted using image processing techniques were compared with expert evaluations, it was determined that the technique provided precise values for the extent of the diseased area with a sensitivity that could not be observed

through visual inspection. The detection of leaf spot disease using image processing techniques is illustrated in Figure 1.

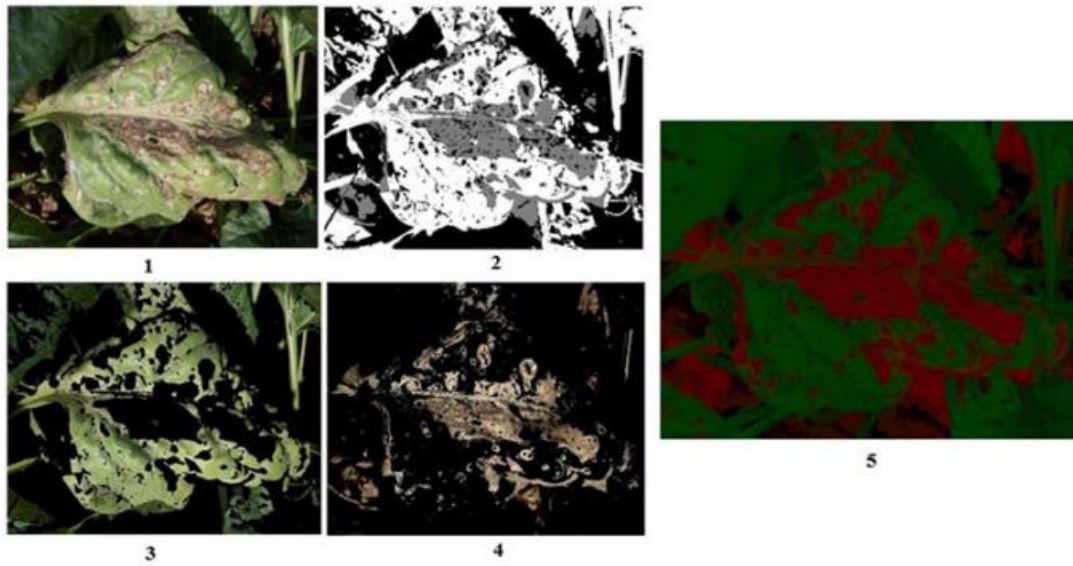


Image 1

Detection of Plant Pests and Pesticide Application

Chen et al. (2021) conducted a study to identify pests in fruit trees and determine areas for pesticide application. In their research, images of pests captured by a drone were sent to an embedded system, NVIDIA Jetson TX2, installed in the orchard via a network. The TX2 system recognizes the development stages and locations of pests in real-time. The locations of pests are then utilized to plan the most efficient route for pesticide spraying. Figure 2 illustrates the areas where pesticide application is needed after the pests have been detected.



Image 2

As seen in Figure 2, after determining the locations of pests, areas within a 5-meter radius from the location of pests, where pesticide application is required, are marked with yellow dotted circles. The red stars are used as coordinate points for positioning and calibration of the drone during each flight.

Monitoring Plant Growth

In a study conducted by Ore et al. (2020), a model was developed for predicting the growth of corn plants, and a growth map was prepared using a drone equipped with Synthetic Aperture Radar (SAR). SAR provided information about changes in terrain height between two flights following the same flight path at different times. In the data collection process with SAR, the researchers initially mounted three corner reflectors in the test area for ground and radiometric calibration. Subsequently, a GNSS base station was placed near the drone's initial position, and GNSS recording was initiated. A circular flight model was chosen to create growth maps. After activating the radar, the drone was flown at the same circular flight route from a height of 120 m on different dates. The reflection images obtained from these circular flights were processed using a back projection algorithm with a 30x30 cm sampling, resulting in the generation of a plant growth map. The corn plant growth maps obtained at three different time intervals are presented in Figure 3.

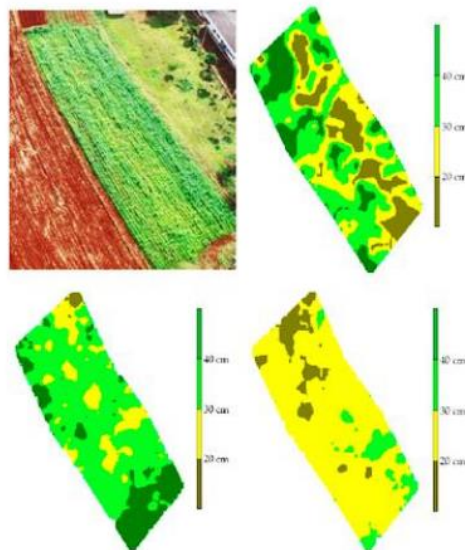


Image 3

Detection of Weeds

In a study conducted by Mattivi et al. (2021) with the aim of determining and mapping the spatial distribution of weeds in corn plants, they utilized a low-cost small commercial drone. They obtained 120 georeferenced photos from a height of thirty-five meters above ground level. The researchers processed the obtained images for weed detection using three different methods: Maximum Likelihood Classifier (MLC), Artificial Neural Network model (ANN) implemented in the OpenCV library in SAGA GIS, and Object-Based Image Analysis (OBIA). The weed maps obtained with these three methods are shown in Figure 4. As a result of the study, weeds in the field were successfully mapped with an accuracy of 99.55% for the

ANN method, 99.50% for the MLC method, and 99.38% for the OBIA method. Additionally, prescription maps for weed management tailored to specific areas were generated from the created maps.

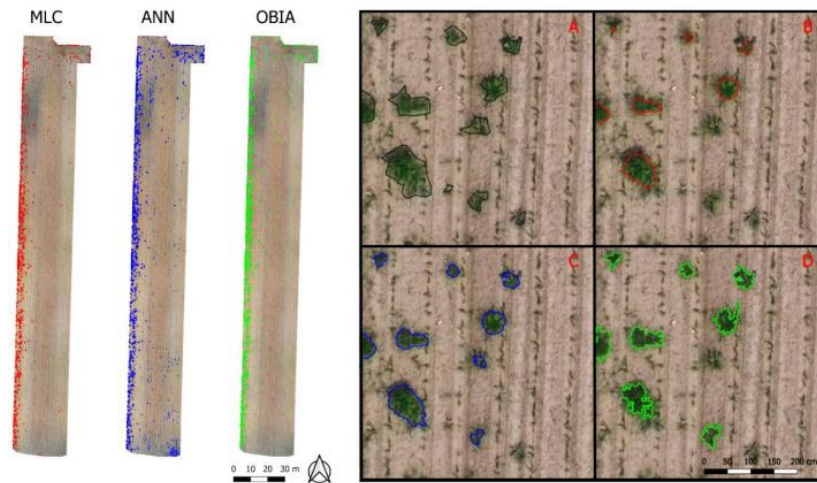


Image 4

In Figure 4, the maps shown on the left were created by first performing semi-automatic classification on the system, where plant, weed, and soil reference data were manually defined. Subsequently, algorithms created with the three methods detected and extracted the features of the manually marked weed reference data, as shown in the map details in Figure 3, and classified them.

2. CONCEPTUAL DESIGN OF UAV

In the selection of configurations, ease of production will be taken as the primary factor, as it is much easier to prevent production errors with simple techniques.

2.1 Wing Configurations

Wing Placement	Advantages	Disadvantages
<p>TOP</p>	<p>High stability. Returns equilibrium by itself with pendulum effect. Ground clearance</p>	<p>Low maneuverability</p>
<p>MID</p>	<p>More stable than bottom placed wing Has more maneuverability than top placed wing</p>	<p>Requires support through fuselage or wings directly mounted on fuselage</p>
<p>BOTTOM</p>	<p>High maneuverability</p>	<p>Unstable. Requires extra control to stay stabilized</p>

Table 3

The payload will be positioned one meter below the aircraft, significantly lowering the center of mass. Mid wing configuration allows the aircraft to maintain the necessary maneuverability when empty. However, when the payload is loaded, the center of mass shifts downward, providing the required stability.


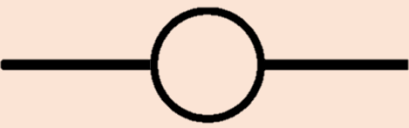

Wing Slope Configurations	Advantages	Disadvantages
 <p>Anhedral</p>	High maneuverability	Low ground clearance Less stable Hard to produce
 <p>Straight</p>	Easy to produce.	Does not have any additional effects
 <p>Dihedral</p>	High stability High ground clearance	Less maneuverability Hard to produce

Table 4

Dihedral was a favorable choice initially, but considering the production difficulties, its benefits were seemed too weak. Therefore, straight wing configuration was selected.

2.2 Motor Placement

The criteria considered in the selection of the propulsion system were system weight, power obtained, and applicability. While weight and power were determined quantitatively, applicability criterion was determined qualitatively based on available resources experiences gained on these systems. 15*5.5 propellers planned to use on all motors.

Motor Configuration	Weight	Vertical Thrust	Horizontal Thrust	Applicability	Total
2+1 – Two tilts and one vertical	2.8	3	2	1	8.8
2+2 – Two tilts and two verticals	2.2	4	2	2	10.2
4+1 – Four vertical and one horizontal	2	4	1	4	11

Table 5

2.3 Tail

Considering the production conditions, the conventional tail type has been chosen as the most robust tail type that can be produced with minimal production error. The tail design is planned to consist of a total of 4 pieces, including the part connected to the carbon plate inside of the fuselage. Also, horizontal stabilizers located above wing level, which prevents turbulent flow from wings.

2.4 Body

The body of the aircraft will be built on top of a carbon plate. The tubes carrying the wings, tail tube, front motor and necessary components will be fixed to this plate by screws or plastic clamps. It should be noted that the external covering of the aircraft serves only a protective function. Also, there will not be any payload inside the body, therefore the fuselage was designed to be thin and elongated to minimize impact on the airflow created by front propeller.

Camera and Drop system both have place under the body. Their location will be determined on manufacturing.

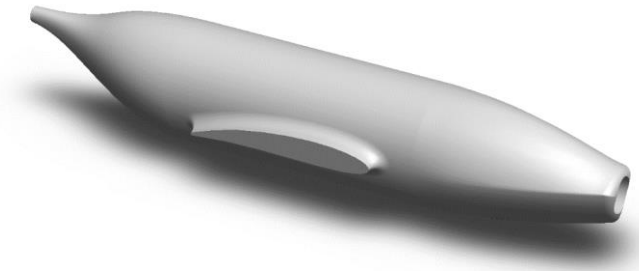


Image 5

Thin, elongated body and soft contours minimizes impact on the airflow created by front propeller.

2.5 Weight Estimation

Component	Pcs/Quantity	Unit Weight (gram)	Total Weight (gram)
SunnySky X4110S-400 Kv Drone Motor	5	165	825.00
Orange Cube Autopilot + ADS-B Standard Carrier Board Set	1	73.00	73
Pixhawk HERE 3 CAN GPS / GNSS WITH M8P	1	50.00	50.00
Raspberry Pi Camera Module	1	12	12.00
HolyBro 433 MHz Telemetry Module	1	20	20
Skywalker 60A ESC	6	63	378
Raspberry Pi 4 Model B	1	50	50.00
Leopard Power 10000 mAh 22.2V 6S 25C Battery	1	1250	1250.00
Tower Pro MG90S Servo Motor	4	13.40	54
Tower Pro SG90 RC Mini 9gr Servo Motor	1	9	9.00
T-Motor 1555 Cw Ccw Propeller	5	24	120.00
Fiberglass	0.13	100	13.00
Carbon Fiber (pipe)	4.5	160	720.00
Carbon Fiber (fabric)	200	0.2	60.00
Cables, screws, 3d printed parts epoxy etc.	1	1900	1900
Adhesives	1	50	50
Total Estimation			5584

Table 6

Based on the preliminary calculations, the weight was determined to be 4 kg. Taking into account the durability of the fuselage, additional components such as motor mounts, wings and adhesives the weight was calculated to be 5.6 kg.

2. 6 Airfoil Selection

NACA 4612 for wings and NACA 0010 for vertical, horizontal stabilizers and winglets have been chosen.

Before choosing the airfoil, cruising Reynolds Number must be determined to perform analysis. According to formula, 0.2m chord length and between 15-20m/s cruising speeds predicted. That gives us a range of between 200,000 and 300,000. Air densities were considered as 1.116 kg/m^3 (Temelli Airfield, 750m, 12 Celsius degrees). Analysis done on XFLR5.

Wing Profile Selection (NACA 4612)

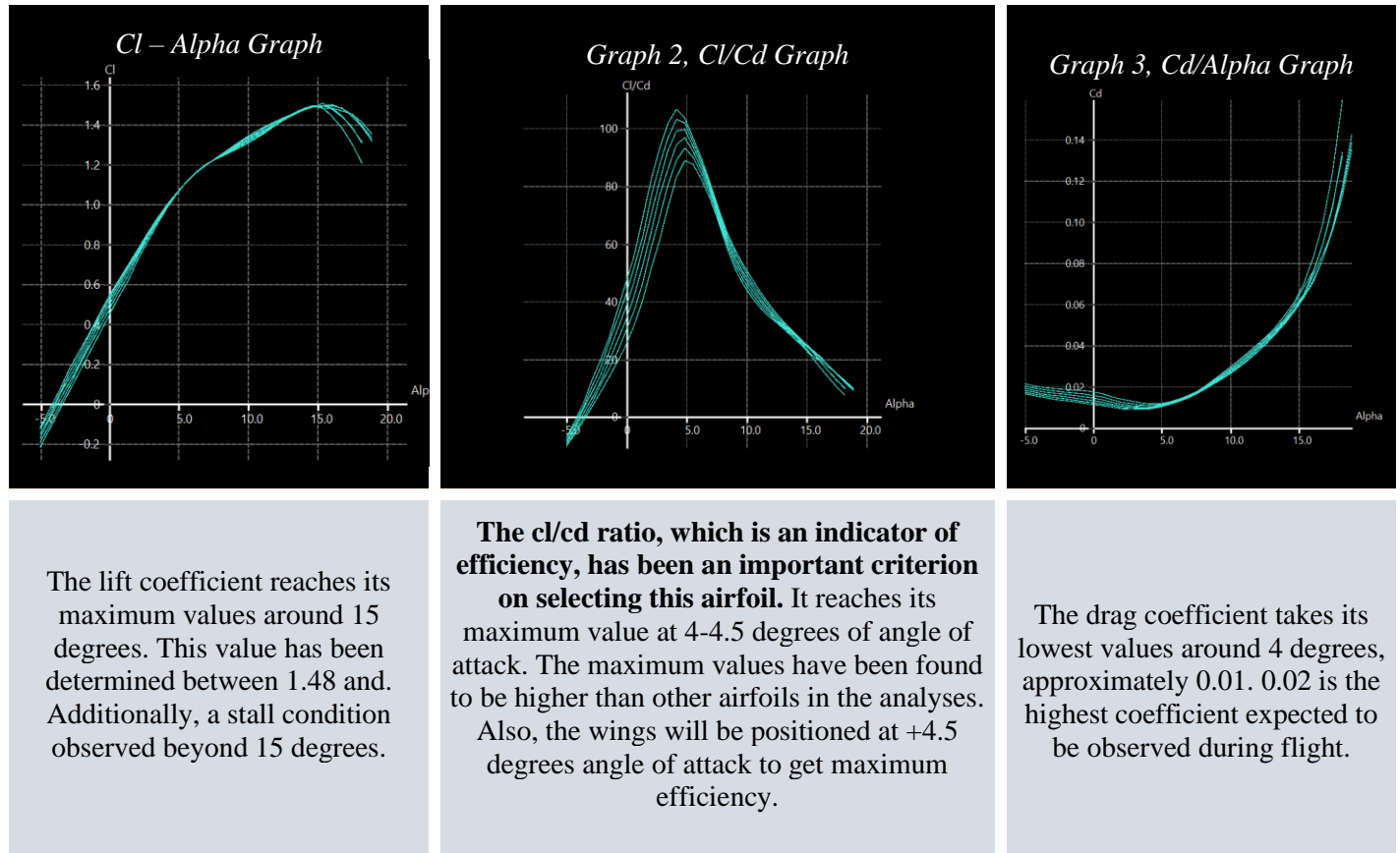
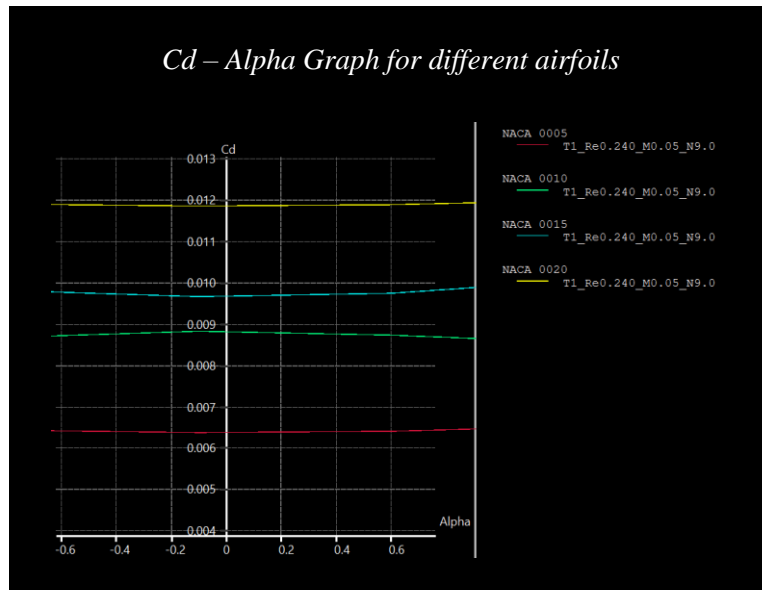


Image 6

Airfoil Selection (NACA 0010)



When selecting wing profiles for the tail and other aerodynamic surfaces, low drag was aimed. Symmetrical NACA profiles were chosen as the wing profile. The effect of the difference in thickness between them on drag was examined.

The graph above illustrates the drag coefficients of different NACA profiles with varying thicknesses. While the values are quite low, the coefficient ratio between the two profiles reaches two. That means two times greater drag force.

Therefore, selection of the thinnest possible profile aimed. NACA 0010 was the thinnest profile could be produced.

Image 7

3. PRELIMINARY DESIGN

3.1 Methodology

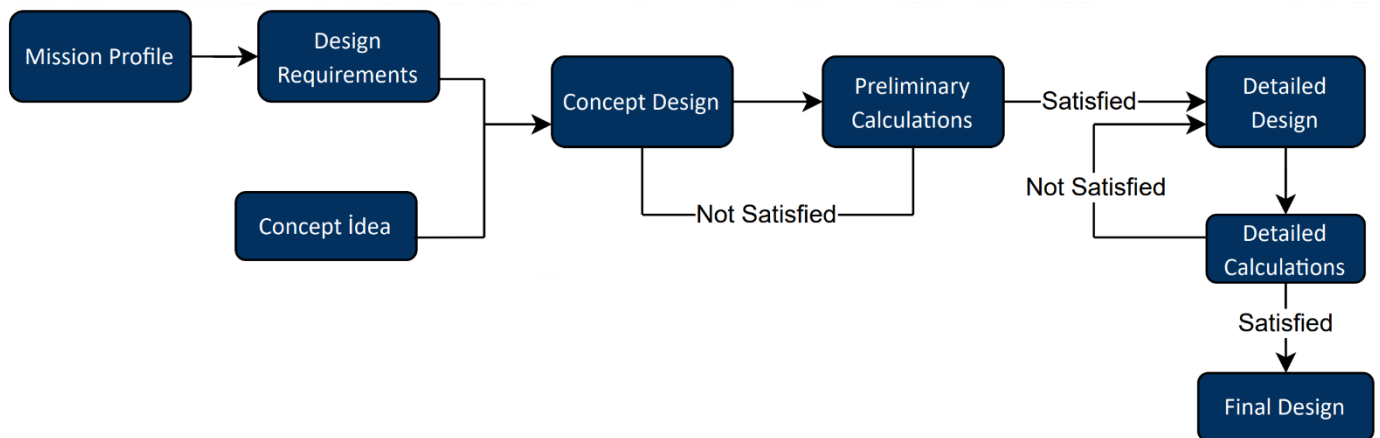


Image 8

3.2 Design-Sizing Trades

While it may seem sufficient for the VTOL vehicle to only be able to perform its missions, having a vehicle that is as lightweight, robust, efficient, and easy to manufacture as possible is a positive situation for both the manufacturer and the user. Therefore, when designing the vehicle, attention has been paid to certain factors, and an effort has been made to strike a balance.

3.3 Aerodynamic Design

The aircraft's aerodynamic structure has been designed entirely for flight during missions, with maximum efficiency achieved during cruise. By positioning it at the front motor-wing level, stability analysis simplified and additional moments by thrust has been neutralized.

3.4 Fuselage

The fuselage has been designed to combine strength, protection from external factors for critical components such as the power unit and the flight computer, and the aesthetic appearance that will give the aircraft its character. This body design also provides efficiency.

Not needing a cargo compartment for external payload storage was a significant advantage in reducing the fuselage size. To keep drag force low, the fuselage was designed to be slim and elongated while maintaining the same volume.

Components have been planned to mount on a carbon plate to ease assembly of flight equipment and connecting elements, to simplify center of mass adjustment, to provide a clean workspace, and to ensure that internal changes do not affect the fuselage.

For stability, it was necessary for the flight computer and the heaviest component, the battery, have to be at the center point of the main wing chord. Therefore, when determining the thickness of the fuselage, the battery, flight computer, and wing connection were initially stacked on top of each other. Then, a circular shape was selected as the optimum shape to encompass them. When the parts were drawn with measurements in the SolidWorks, it was found that a circle with a diameter of 16cm was sufficient, and the fuselage diameter was set at 16cm.

Locating the battery bottom of the fuselage and making it possible to freely positionable on the longitudinal axis increases stability and provides flexibility while adjusting the center of mass.

3.5 Wing Sizing

When determining the chord length and wingspan of the wing, a balance was struck between strength and efficiency. A high aspect ratio yields higher efficiency, which requires a decrease in chord length and an increase in wingspan. However, reducing the chord length decreases the diameter of the carbon supports within the wing, while increasing the wingspan also increases the stress these slender supports would be subjected to. The balance between these two factors was achieved by designing wings with a chord length of 25cm and a wingspan of 2 meters to fit the 16cm diameter fuselage.

3.6 Understanding Slung Load

Slung load is a distinct type of load compared to standard fixed loads. It is positioned outside the fuselage and has the freedom to move, resulting in a significantly higher drag force. Additionally, it is crucial to discuss and predict its movement during flight in order to prevent any unexpected maneuvers or stall condition.

The inertia of the load will cause a delayed response due to its free movement. It is assumed that the rope connecting the load is rigid. Therefore, in vertical flight, the impact can be disregarded. However, during horizontal flight, especially during turns, appropriate approaches were developed, and the effects on the aircraft must be anticipated.

Also, it is required to have at least a 1-kilogram payload, which equals 25% of UAV's empty operating weight.

Due to its own inertia, a slung load will experience a slight delay before it starts swinging outward. This swinging motion will exert an outward force, pulling the aircraft from the point to outside where the load is attached. While mounting tail on body, possible twists and stretches will be considered.

3.7 Stability and CFD Analysis

After determining the weight, configurations, and wing profiles, a preliminary model was created for stability analysis and perform performance calculations, while considering the wing area and production capabilities. The stability of the aircraft was analyzed within the range of -5 to +9.50 degrees of angle of attack

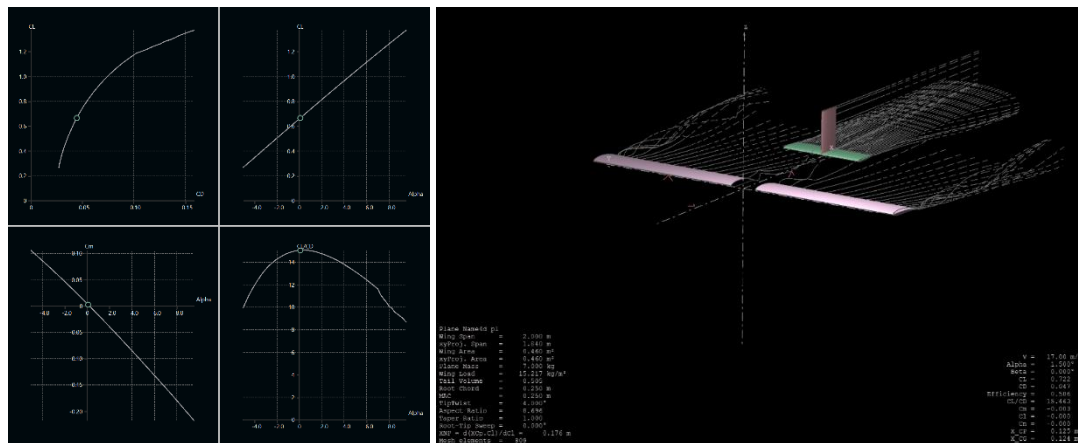


Image 9

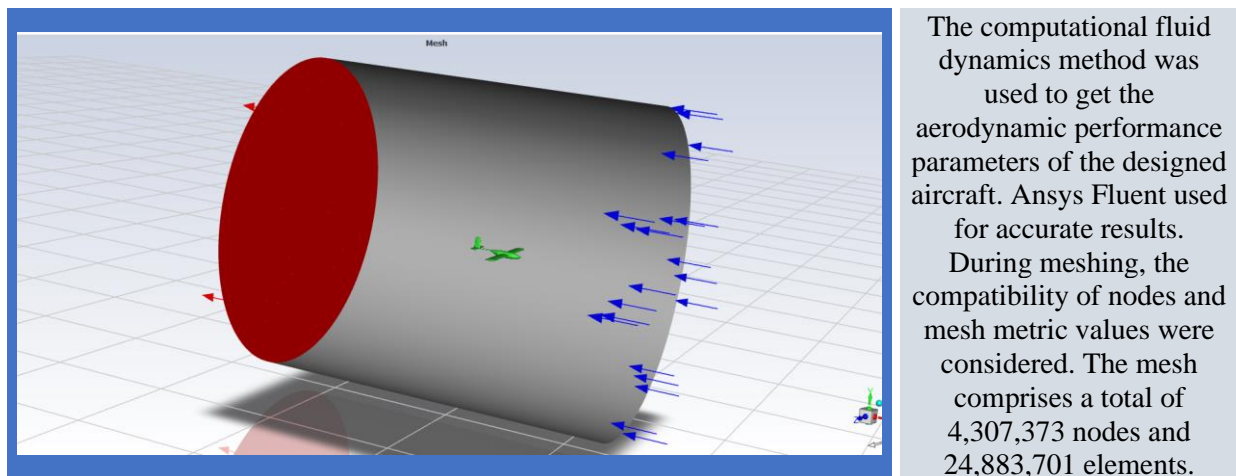
(In order to top left to bottom right) CL/Cd , CL/α , Cm/α and CL/Cd alpha graphs and essential information.

Negative-sloped moment coefficient graph indicates that the aircraft is dynamically stable [1]. Additionally, the same graph shows that the aircraft maintains stability about 1.5 degrees. The CL/Cd ratio reaches its peak values around 0 degrees, which corrects the previous Reynolds number prediction made during the airfoil selection process when placing the wing at +4.5 degrees. The wing area was designed as 0.46 m^2 [3]. While calculating the stall speed, maximum CL value taken from the graph, but the aircraft can fly at lower speeds, as is well known. Therefore, during the testing process, real stall speed will be determined practically in detail.[2]



Mesh view and Mesh Properties Table

Image 7



Dimension of the enclosure determined while considering size of aircraft

Image 10

Boundary Conditions Used in the Analysis:

- Independent of time, gravity and temperature variations were neglected.
- The k- ω turbulence model was employed.
- Considering the altitude of the aircraft, density was taken as 1.14 kg/m^3 .

The analysis results indicate a drag coefficient value of 0.062 and a drag force of 4.17 N. The lift coefficient for zero angle of attack has been calculated as 0.87.

drag_coefficient	0.062734711
drag_force	4.1785892 [N]
lift_coefficient	0.87237344
lift_force	58.106432 [N]

4. Estimations

4.1 Wing Area and Wing Load

Variables	Formula [3]	Result
$L = W = 68.67 \text{ N}$ $\rho = 1.14$ $C_L = 0.87$ $V^2 = 289$	$S = \frac{2L}{\rho V^2 c_L}$	$S = 0.4779 \approx 0.48 \text{ m}^2$
	$W_{loading} = \frac{W}{S}$	$W_{loading} = 143 \text{ N/m}^2$

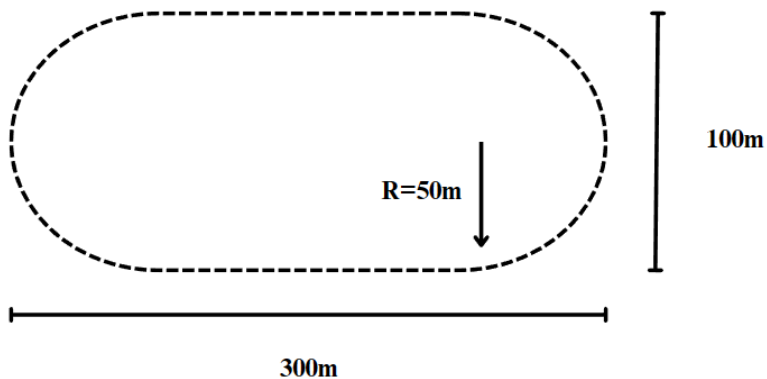
Table 8

4.2 Stall Speed Calculation

Variable	Formula [3]	Result
$C_{L_{max}} = 1.37$	$V_s = \sqrt{\frac{2W}{\rho S C_L}}$	$V_s = 13.57 \text{ m/s}$

Table 9

4.3 Bank Angle Calculation



Flight route simplified like this stadium shape to ease calculations while turning.

Centrifugal Force	Formula [3]	Result
$F_m = \frac{mv^2}{r} = 40.46 \text{ N}$	$\alpha = \arcsin\left(\frac{F_m}{L}\right)$	$\alpha = 36^\circ$

Table 10

4.4 Angle of Attack Calculation

Lift Required	Cl required on banking [3]	Result
$L = \sqrt{68.67^2 + 40.46^2} = 79.7N$	$c_{L_t} = \frac{2L}{\rho V^2 S} = 1.05$	<i>Cl-alpha graph</i> shows that the desired value is obtained at a +5.5-degree angle of attack.

Table 11

4.5 Thrust Available Calculations

Thrust values could be determined from table below which was provided by manufacturer.

Prop (inch)	Voltage (V)	Amps (A)	Thrust (gf)
15*5.5	22.2	1.9	500
		3.2	750
		4.9	1000
		6.9	1250
		9.2	1500
		11.4	1750
		14.2	2000
		18.8	2430

Table 12

Thrust values provided by manufacturer [4]

	Motor Quantity	Max Thrust Per Motor (gf)	gf to N Conversion ratio	Total Force (N)
Vertical	4	2430	0.981	95.35
Horizontal	1	2430	0.981	23.84

Table 13

Maximum Thrust Available

4.6 Maximum Cruise Speed

Variables	Formula [3]	Result
$T = D = 23.84N$ $C_d = 0.063$ $S = 0.4m^2$	$V = \frac{2D}{\rho S C_d}$	41m/s

Table 14

5. Power Consumption

5.1 Propulsion

Work completed in a given length of time is called power. Multiplying the necessary thrust force by the cruise speed yields the power needed for cruising. When the airplane is cruising, the drag force it experiences is equal to the necessary thrust force.

For cruise flight

$$P_{cruise} = T_{cruise} \times V_{cruise}$$

$$T_{cruise} = \frac{1}{2} \rho V^2 S C_D$$

$$T_{cruise} = 3.88 \text{ N}$$

$$V_{cruise} = 17 \text{ m/s}$$

$$P_{cruise} = 65.96 \text{ W}$$

For vertical take off

Based on momentum theory, the power needed for a rotary wing aircraft's vertical takeoff and landing is calculated for the rotor disk. Consequently, the following formula is used to determine how much power the airplane needs to have at the instant of vertical takeoff:

$$T_{TO} = K_T W_{TO}$$

$$P_{TO} = \frac{T_{TO} V_{TO}}{2} \left[\sqrt{1 + \frac{2 * T_{TO}}{\rho * V_{TO}^2 * A_{propeller}}} \right]$$

The aircraft was found to have a vertical take-off speed of 3 m/s and a take-off weight of 5 kg. The necessary thrust value during vertical take-off was selected to be 20% greater than the entire take-off weight in order to provide reasonable passing maneuvers.

It follows that is found.

$$P_{TO} = 868.65 \text{ W}$$

5.2 Control Units

Component Name	Operating Current	Op. Voltage	Power Consumption
Pixhawk Orange Cube	2,5 A	4.1V – 5.7V	14 W (All servos included)
Raspberry Pi 4 Model B	2,5 A – 3 A	5,0 V– 5,2 V	6 W – 10 W

Table 15

Control Units Power Specifications

Flight power consumption varies according to the flight modes, with vertical modes requiring the aircraft to generate lift using vertical motors. As known from performance calculations, vertical modes tend to consume more power. In flight scenarios and configurations, particular attention is paid to minimizing the flight time in vertical modes. Also, in scenarios where image processing is not used, the Raspberry Pi operates in a low-power mode.

6. DETAILED DESIGN

6.1 Dimensions

Total Length	1.38m	Vertical Stabilizer Area	0.0375m ²
Wingspan	2m	Horizontal Stabilizer Area	0.075m ²
Fuselage Length	0.825m	Empty Operating Weight	5.5kg
Fuselage Diameter	0.16m	Payload Capacity	1.5kg
Wing Area	0.46m ²	Maximum Operating Weight	7kg

Table 16

6.2 3D Drawing Package

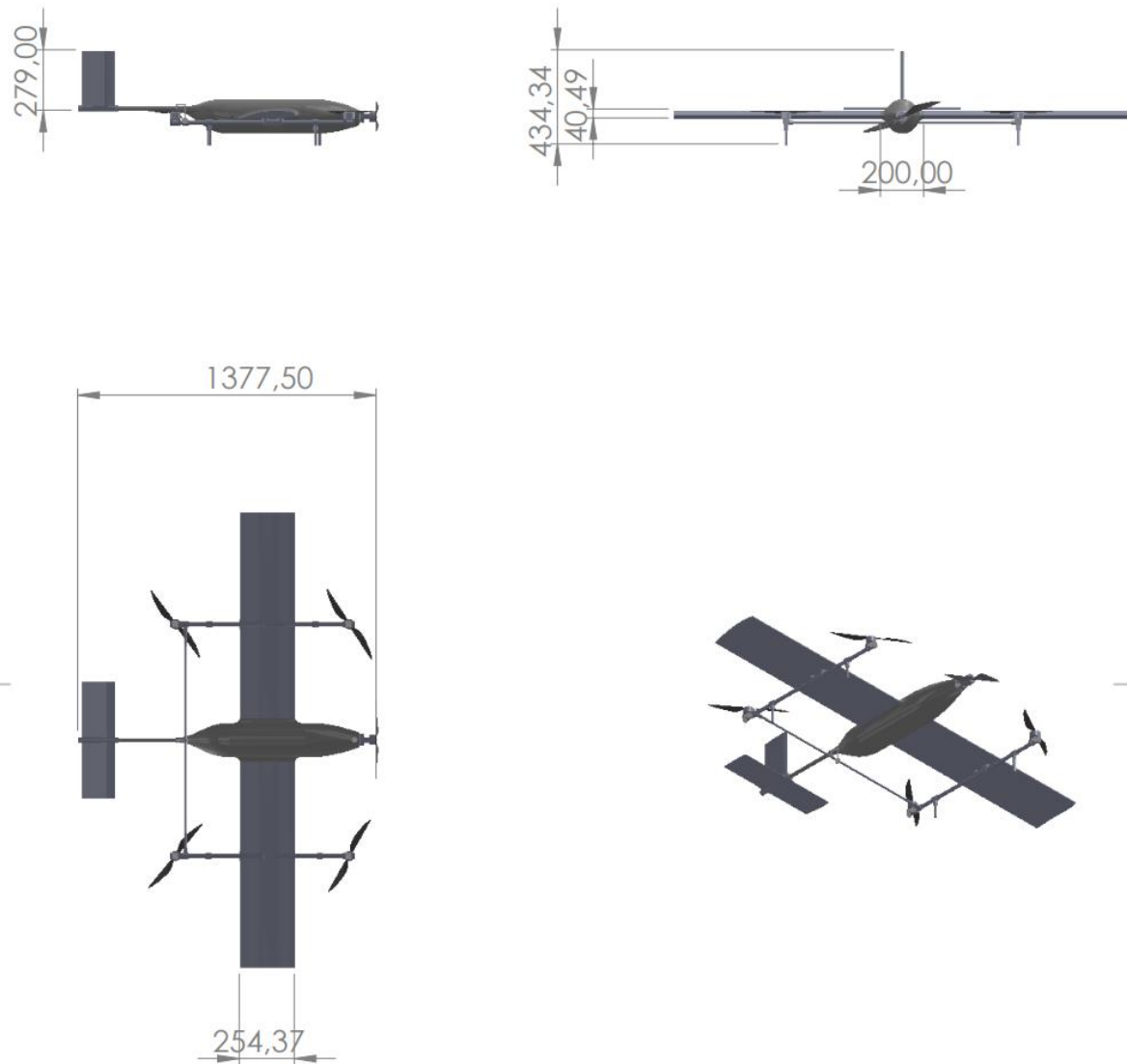


Figure 1

6.3 Weight and Balance

When determining the aircraft's center of gravity, fly in drone mode considered. The center of the wing's chord was chosen for center of gravity. This makes the forces acting on the vertical motor support tubes symmetrical. To verify the center of gravity and ensure that the tube is mounted properly, a special screw was placed on the connection part. The aircraft can be hung from these screws to adjust the center of gravity precisely.

Component	Mass (kg)	Weight (N)	Offset (m)	Moment (Nm)
Main Fuselage	0.375	3.67875	0.150	0.55
Nose Fuselage	0.180	1.7658	-0.260	-0.46
Horizontal Thrust Module	0.250	2.4525	-0.300	-0.74
Raspberry Pi and Camera Module	0.070	0.6867	-0.220	-0.15
Cube Orange	0.085	0.83385	0.125	0.10
Vertical Thrust Module	1.060	10.3986	0.125	1.30
GPS	0.050	0.4905	-0.025	-0.01
Telemetry Module	0.012	0.11772	0.500	0.06
Battery	1.250	12.2625	0.100	1.23
Tail Module	0.360	3.5316	0.770	2.72
Wings	0.785	7.70085	0.105	0.81
Vertical Thrust Module Support Pipe	0.190	1.8639	0.125	0.23
Carbon Plate	0.175	1.71675	0.150	0.26
EPP Foam	0.050	0.4905	0.300	0.15
Back Support Tube	0.055	0.53955	0.350	0.19
Back Support Tube Connection	0.045	0.44145	0.350	0.15
Landing Gears	0.300	2.943	0.125	0.37
Fuselage - Plate Connection	0.080	0.7848	0.125	0.10
Front ESC	0.063	0.61803	-0.030	-0.02
Total Mass	5.435	Total Moment		6.84

Table 17

*Reference is wing's leading edge

*Designed center of mass has a moment of 6.74 Nm on the reference point

*Aircraft is symmetrical, z axis could be neglected

*For longitudinal stability, y axis also could be neglected

*Extra adhesive masses neglected

The table shows that component's total moment is nearly equal (0.1Nm difference) to designed center of mass' moment. It means that the stability predictions should be precise.

6.4 Body

The aircraft's assembly point, which is the fuselage, includes of three main components and their connections. The fuselage and the nose section are made from carbon fiber, while the third is a carbon plate prepared to fit inside the fuselage. The fuselage is divided into two parts from the nose section. After fitting the carbon plate into the rear section, the front section is fixed to both carbon plate and main fuselage to complete body. To provide access to components inside the fuselage, a top hatch has been opened.

3D printed parts have been used for the front motor connection, rear tail connection, and plate-fuselage connection. Using M5 nuts and bolts for connections (except for the hatch and front motor connection) and using exact parts for the plate-fuselage connection make maintenance and repair work easier.

6.5 Wing and Other Aerodynamic Surfaces

The aircraft's aerodynamic surfaces are made of three main materials: EPP foam for the filling, carbon pipes for structural support. The pipes at the root wing and tip wing can intertwine each other to create telescopic structure. Removable wingtips reduce occupied space during transport and allows the aircraft to fly in the most suitable configuration for different missions.

3d printed custom servo slots has been prepared for servos which controls aerodynamic surfaces. In case of any failure a new servo can be replaced easily.

6.6 Structural Frame

The entire structural frame of the vehicle is made of carbon fiber, and the connection components are custom-printed parts. When planning the connection points, attention has been made to preserve the vehicle's rigid structure.

6.7 Tail

The tail of the aircraft is made from 3d printed base and spars, carbon fiber for supports and fiberglass tape for covering. It connects to body from two points. First one is a ring that fixed on body, the second one is a vertical screw that prevents tail from twisting and slipping on longitudinal axis. Only one screw was used, so it can be mounted less than a minute correctly.

6.8 Landing Gear

The landing gear has been designed very simple to minimize weight due to vertical takeoff and landing. It has been made of 3d printed parts and carbon pipes mounted on body to minimize vibrations while taking-off.

6.9 Release System

The release system has been positioned at the center of mass of the aircraft and designed to withstand the stress during flight.

6.10 Anticipating Effects of the Slung Load

During manual test flights, the behavior of the slung load was examined, maneuvers to minimize the effect were performed, and integrated into autonomous flight. Winglets were added to the wingtips to increase efficiency and horizontal stabilizer surface area.

7. Avionics

Avionics is the electronic systems in aerospace platforms (aircraft, satellites, etc.) that carry out specific operations dependent on electronic and electro-mechanical parts. For example, navigation, control, display, management of multiple systems, and communication are contained in these types of operations. To maintain flight and other exertions, avionics systems, and subsystems should be created and integrated by considering the mission requirements. There are three main systems that are Propulsion System, Control System, and Power System to perform the missions. In addition, two subsystems are needed for detecting the target and releasing the payload, which are Communication System, Target Detection System and Payload Release System. The avionic system design of a typical VTOL vehicle comprises a microcontroller, flight control computer, battery, electronic-speed controller (ESC), brushless electric motors, and servo motors.

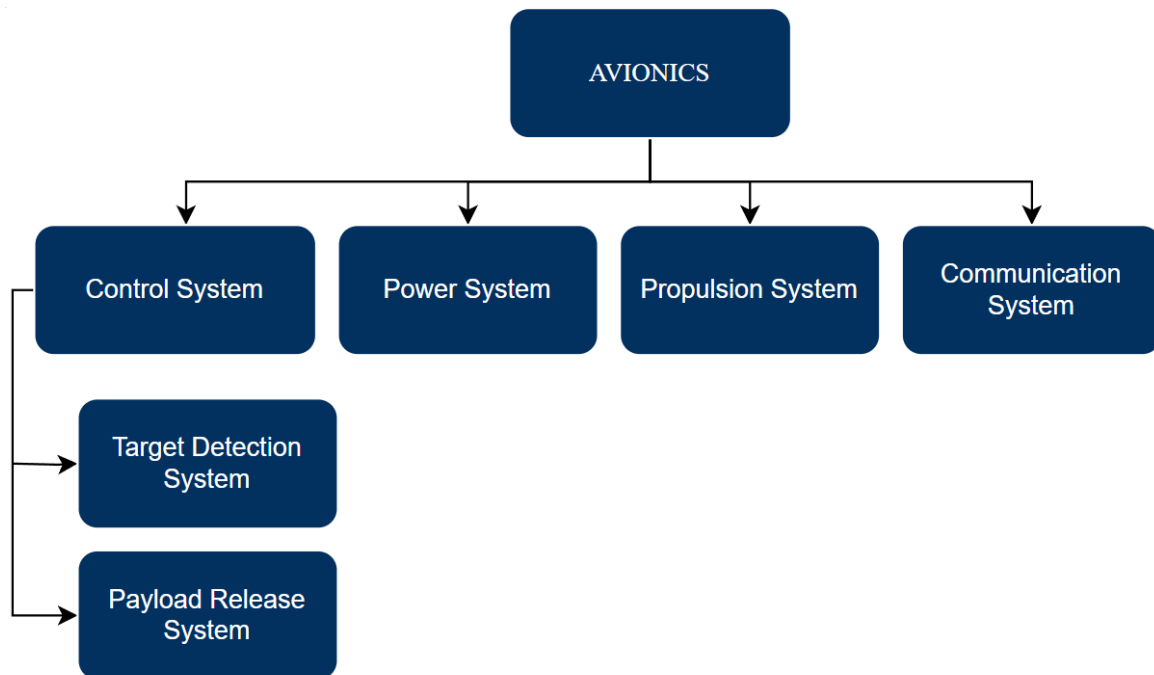


Figure 2

7.2 Component Selection

The relationship between systems and components assumes a significant extent. Within this framework, the selection of components emerges as a critical decision, as their capabilities and characteristics fundamentally define the system's overall efficiency and capacity. To design a competitive VTOL, the decisions were made carefully.

7.3 Microcontroller

Microcontrollers are small, self-contained computing devices designed to perform specific tasks or control various systems, optimized for real-time operations, and are commonly used in embedded systems. The third mission requires target detection which is a real-time application. Thus, there must be a microcontroller and a camera module to have real-time images while the VTOL is on the mission flight. There are two microcontrollers that are able to achieve this task.

7.3.1 Option 1: Raspberry Pi 4 8GB

Raspberry Pi series is a popular development card series which has numberless libraries and applications. Also, it has an Operating System based on Linux. It gives a high image processing performance with low power. The control card is compatible with Python and OpenCV libraries.



7.3.2 Option 2: Jetson Nano 4GB

Jetson Nano is a microcontroller developed by Nvidia. Image processing application performance is much higher, however, at high use of power. It can provide high resolution-images. Python and OpenCV libraries are also available with configurations.



Microcontrollers	Performance	Image Processing	Power Consumption	Weight
Raspberry Pi 4 8GB	+	+	+	+
Jetson Nano 4GB	+	+	-	-

Table 18

Comparison of the Microcontrollers

Raspberry Pi 4 have been chosen. Because, power consumption is an important requirement and Raspberry Pi 4 is cheaper and lighter [5]. High use of power for the microcontroller can affect the flight time. The second motivation is that Raspberry Pi 4 has been more widely experienced through individual projects.

7.4 Flight Controller

Flight controller is a computer that has flight sensors integrated on the base board such as accelerometer, magnetometer, gyroscope, barometer to collect the data to estimate the aircraft's location, 3D angular speed and acceleration, vertical speed and direction, altitude etc. and produces signals to control the aircraft. Many flight controllers match the mission requirements which might be suitable for VTOL flight scenario. However, the optimal options are discussed.

7.4.1 Option 1: Pixhawk Cube Orange

Orange Cube is a common and advanced flight controller. The card is equipped with the STM32H753[6] processor for optimal performance, while the STM32F103[6] serves as the failsafe processor, ensuring reliable data transfer at high speeds. Moreover, it has a high-resolution IMU (Inertial Measurement Unit) sensor combination and proves highly suitable for applications requiring precise control.[7]



7.4.2 Option 2: Pixhawk 2.4.8

Pixhawk 2.4.8 is the same product of the manufacturer as Orange Cube. STM32F427 powered the card and back-up processor is STM32F103 which is the same auxiliary processor of the Orange Cube. When it comes to the IMU, Pixhawk 2.4.8 has general-purpose and basic sensors with the exception of the barometer.[8]



Flight Controllers	Frequency, Data Transfer	Power Consumption	Sensor Accuracy	Open-Source Code
Pixhawk Cube Orange	+	Neutral	+	+
Pixhawk 2.4.8	Neutral	+	-	+

Table 19

Comparison of the Flight Controllers

The decision to integrate the Orange Cube as the controller card, combined with a GPS module, was motivated by its high-precision IMU, exceptional data transfer speed and frequency. While the Pixhawk 2.8 presents an alternative option due to its lower power consumption in comparison to the Orange Cube, the design prioritizes high-performance attributes for the controller component. The difference in power consumption is negligible according to the ratio of power usage to the performance achieved. Both control cards fully support the Ardupilot autonomous flight software package, facilitating installation and compatibility for designated application. By the features of the Orange Cube, achieving high performance and precision in VTOL system design were aimed.

7.5 Battery

Batteries are electrochemical devices that store and release energy in the form of electrical power. If voltage is applied, the voltage between the poles of the battery increases, because of chemical reactions within the battery's cells which store the potential energy. Therefore, the battery supplies current when connected to a circuit. Although there are various types of battery such as Ni-Cd, Ni-MH, Ag-Zn, Li-Ion and Li-Po. Li-Po battery was selected for the reason of the high energy density compared to its unit weight.



Model	Leopard Power 10000 mAh 6S Li-Po Battery
Battery ampere value	10000 mAh
Continuous Discharge Current	25C (250.0A)
Burst Discharge Current (10 sec)	50C (500.0A)
Voltage	22.2 V
Weight	1250 g

Table 20

7.6 Electric Motors

Electric motors are electromechanical components, converting the electric power into mechanical power by using magnetic fields. There are two types of electric motors; brushed and brushless motors. Brushless DC motor is selected to perform the thruster task. Completed literature researches reveal that brushless motors are reliable, efficient and quieter and can run at high rotary speed and torque.[9]



Model	Sunnysky X4110S-400 Kv drone motor
Engine Kv	400 Kv
Max Trust	3720 g
ESC	40-60 A
Weight	165 g
Suggested Propellers	15 * 5.5 / 16 * 6/18 * 6.1 / 17 * 5.8

Table 21

7.7 Electronic Speed Controller

Electronic-Speed Controller is an electronic circuit that controls the RPM (Revolution Per Minute) of an electric motor by sending voltage signals in order. The main criteria choosing the component is that ESCs must have the ability to perform in the maximum operating current range of the motor. In addition, the brushless motor manufacturer's suggested ESC current interval is 40A-60A. The presence of a Battery Eliminator Circuit (BEC) in ESCs is crucial, as this feature helps maintain a stable power supply for the flight computer that drives the servo motors.



Model	SkyWalker ESC 60A Brushless Motor Speed Controller
Battery Type	Lipo: 2S-6S
Output	60A (withstands up to max 80A and less than 10 seconds)
Weight	63 g
BEC	Equipped

Table 22

7.8 Servo Motors

Servo motors is an actuator which contains an electric motor, an electronic driver and gears to provide the angle at high precision. The principle of the servo motors is to determine the location in closed loop and exert feedback to make the arrangements. 4 servo motors are used to actively control the flight surfaces to make maneuvers and only one is equipped to release the payload.



Model	Tower Pro MG90S Micro Servo Motor
Operating voltage	4.8 V - 6.0 V
Stall torque	1.8 kgf.cm (4.8 V), 2.2 kgf.cm (6V)
Weight	13.4 g

Table 23

7.9 Telemetry

Aircraft must communicate flight parameters to the ground station during flight. To fulfill this requirement, the communication module needs to be integrated into both the ground station and the aircraft. The performance of the telemetry system is defined by characteristics such as data transfer speed, range, and the frequency it operates on.



Model	Holybro Telemetry Radio
Frequency	433 MHz
Range	300 m

Table 24

7.10 Power and Propulsion System

In the guideline of the values obtained as a result of the performance calculations, components selections were made. The VTOL aircraft's power source is a Li-Po 6S 10000mAh 22,2V battery which, considering the operating voltages, is connected to the microcontroller, ESCs, the flight controller by low resistance power wires. In the aircraft, ESCs drive the brushless DC motors and the flight controller transmits the power to the servo motors. LM2596 regulator regulates the high voltage from the battery to provide a stable 5V 2.5A output, ensuring the proper operation of the Raspberry Pi. The Orange Cube flight computer is equipped with an integrated circuit element that includes power regulation. Additionally, the power supply to the ESCs is directly connected to the battery without any need for modification, however, considering the amount of maximum ampere that power cables can carry.

Flight power consumption varies according to the flight modes, with vertical modes requiring the aircraft to generate lift using vertical motors. As known from performance calculations, vertical modes tend to consume more power. In flight scenarios and configurations, particular attention is paid to minimizing the flight time in vertical modes. Also, in scenarios where image processing is not used, the Raspberry Pi operates in a low-power mode.

For the Propulsion System, the estimated take-off weight's 7 kilograms and the thrust should be higher of the weight to accelerate. The 4-rotor Quadcopter was selected for vertical thrust order, because provides more stability, thrust range and applicability. While on cruise flight, the horizontal thrust is provided by one motor. As a result of research 15*5.5 propellers will be mounted on motors due to its efficiency. Considering the system compatibility, the each vertical 4xSunnysky X4110S-400 Kv motors are driven by 4xSkywalker 60A ESC, like so, the cruise motor 1xSunnysky X4110S-400 Kv is driven by 1xSkywalker 60A ESC either. A total of 5xTower Pro MG90S Micro Servo Motor will be used to be used in 2 ailerons, 1 rudder, 2 elevators, to ensure the movement of the control surfaces, and 1 load release system by converting the signal coming from the driver into a mechanical movement.

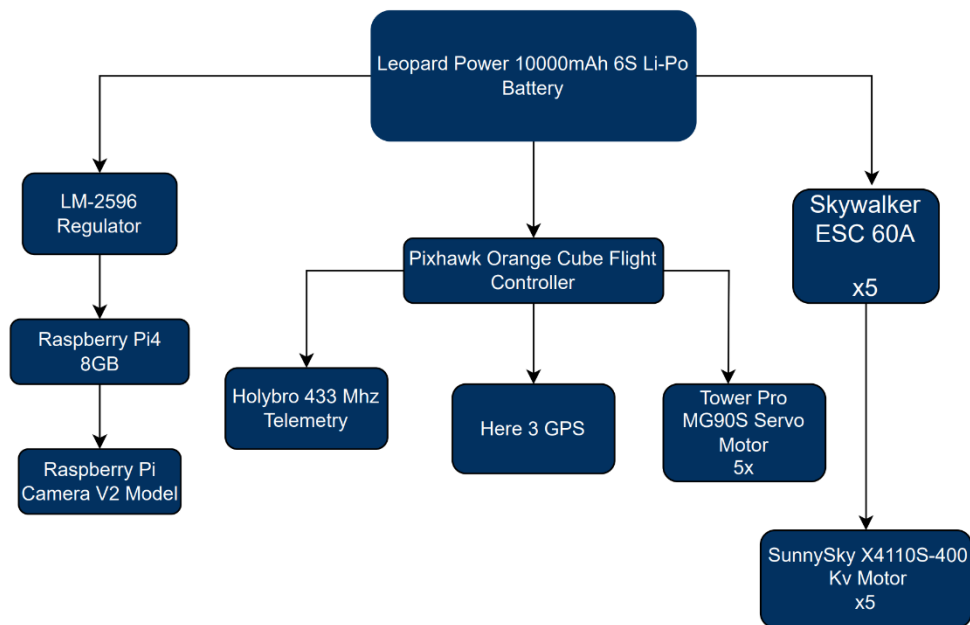


Figure 3

8. Computer Vision and Target Detection System

On the third mission, the payload must be released on the target location area after completing 5 laps by the aircraft. Computer vision will be used for detecting the target. Computer vision is a discipline within computer science that focuses on empowering the computers to identify objects in images and videos. Computer vision seeks to enable computers to perform and automate tasks which are named image processing. In image processing, Python and OpenCV libraries are preferred to be used on the Raspberry Pi 4 microcontroller unit and Raspberry Pi Camera V2 due to their performance, speed, trustworthiness and compatibility. Similarly, by utilizing the DroneKit library and applying the image processing algorithm, it enables the vehicle to perform autonomous flights. The image processing algorithm consists of 3 main parts, which follow the detection of all potential targets, the scanning process and the transformation of coordinates.

8.1 First: Potential Target Detection

This section pertains to the detection of shapes in the image from the camera, which have four continuous edges and boundaries. It involves the application of functions such as edge detection[11], contour finding[12], contour area calculation[13], and contour approximation[13] for this purpose. Additionally, it applies a filter, incorporating altitude, ground angle, and the camera's Field of View (FoV)[14] values. This enables the identification of rectangular targets with approximately known areas and the subsequent application of a filter.

8.2 Second: Scanning Process

The perspective transformation matrix of the identified potential targets is computed, and the image is subsequently cropped from the screen[15]. Following this, functions such as line and circle detection are applied to the cropped image to scan whether the desired conditions are met. Based on this evaluation, the target is confirmed.

8.3 Third: Coordinate Transform

Once the desired target is detected and scanned based on specific features, it is confirmed if it meets the criteria. The position of the confirmed target on the screen is determined by considering the diagonal intersections of its shape. Using IMU, camera, and altitude information, an estimation of the target's position on the ground relative to the aircraft is made.

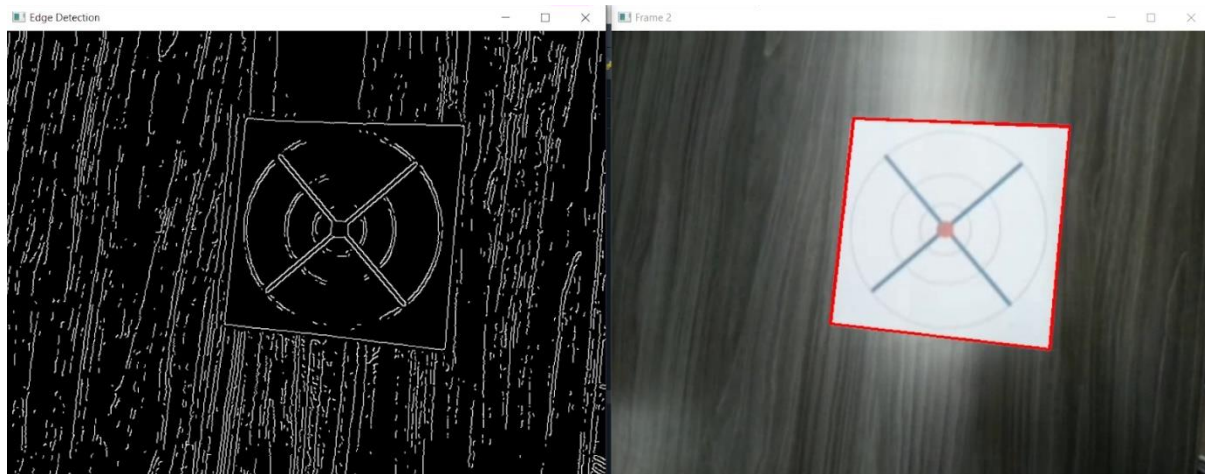


Image 11

Screen image from image processing algorithm-1

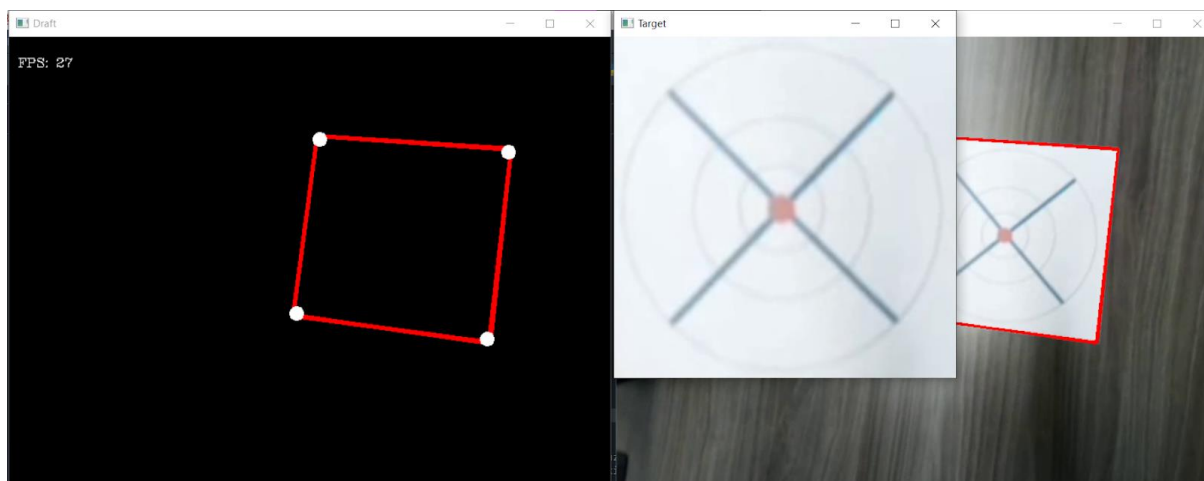


Image 12

Screen image from image processing algorithm-2

9. Control System and Units

The control system plays a pivotal role in managing the flight parameters of the vehicle, analyzing environmental data, and providing precise instructions to the motors and control surfaces. Its primary function is to ensure flight stability and optimize maneuvering capabilities, achieved through the use of PID (Proportional-Integral-Derivative) closed-loop control algorithms. This system is also responsible for seamlessly managing fixed-wing VTOL transitions and facilitating smooth transitions between different flight modes of the aircraft. Moreover, it empowers the execution of autonomous missions. The control system comprises three key units:

9.1 Flight Controller

Within the Control System, the Pixhawk The Cube Orange serves as the flight controller. This central component is responsible for overseeing the vehicle's flight parameters, gathering crucial environmental data, and issuing commands to the motors. Additionally, it plays a crucial role in ensuring the safety of the project by implementing fail-safe measures. The Pixhawk The Cube Orange offers several essential features and responsibilities

Processing Power and Speed: This controller boasts exceptional processing power and rapid data processing capabilities, enabling real-time analysis of environmental data and swift decision-making.

Sensor Integration: The flight controller integrates a range of sensors, including GPS, IMU (Inertial Measurement Unit), barometer, and magnetometer, enabling precise determination of the vehicle's position and orientation.

PID Control Algorithms: Utilizing PID (Proportional-Integral-Derivative) control algorithms, it effectively maintains flight stability and optimizes maneuverability, ensuring smooth flight and responsiveness to control inputs.

Fail-Safe Features: The flight controller recognizes various fail-safe scenarios and takes automatic actions to mitigate them. For example, it can initiate a "Return to Home" (RTH) mode when radio communication is lost or ensure a safe landing when the battery level becomes critically low.

Flexibility and Customization: The Pixhawk The Cube Orange is highly adaptable to different flight modes, allowing for user customization, and ensuring the project meets various requirements and scenarios effectively.

9.2 Companion Computer

The Control System incorporates the Raspberry Pi 4 Model B as the companion computer. This component is crucial for autonomous orientation by capturing real-time images of the flight area and performing target detection, referred to as the Target Detection System. The Raspberry Pi 4 Model B offers the following functionalities:

Autonomous Orientation: The Raspberry Pi 4 actively captures real-time images from the aircraft's surroundings and employs image processing algorithms, including OpenCV (Open Source Computer Vision Library). This empowers the vehicle to monitor its surroundings, detect targets, and focus on specific locations, thereby enabling autonomous flight.

High-Resolution and Performance: High-Resolution and Performance: The Raspberry Pi 4 Model B's ample processing power handles high-resolution images efficiently, ensuring the aircraft accesses clear and detailed information.

Connectivity and Communication: Serving as a communication hub, the Raspberry Pi facilitates control and communication with the drone through DroneKit and the MAVLink protocol. It also acts as a vital interface for transmitting data from the Raspberry Pi to the flight controller, enabling essential communication.

Flexibility and Expandability: The Raspberry Pi allows for project customization and adaptability to diverse applications. It ensures the project remains compatible with future updates and expansions.

9.3 Ground Station

The ground control station is a pivotal element in our project, serving as the command-and-control center for the entire unmanned aerial system. Its role is multifaceted, allowing operators to exercise precise control over the vehicle's behavior, monitor vital flight parameters, and execute mission planning. The ground station is designed to facilitate two-way communication, enhancing remote vehicle control and ensuring seamless interaction with the airborne platform. Its primary functions and features are outlined below:

Flight Parameter Monitoring: Operators utilize the ground control station to continuously monitor the vehicle's flight parameters, including altitude, airspeed, GPS coordinates, and various sensor data. This real-time monitoring empowers operators to maintain situational awareness and make informed decisions during the flight.

Mission Planning: One of the key functions of the ground station is mission planning. Operators can define specific flight missions, including waypoints, flight paths, and various tasks to be executed by the vehicle. The ground station provides an intuitive interface for designing and optimizing these missions to achieve project objectives efficiently.

Two-Way Communication: Two-way communication is fundamental for maintaining control over the vehicle. The ground station acts as a communication hub, enabling operators to send commands to the vehicle and receive crucial telemetry data in return. This bidirectional communication ensures real-time adjustments and decision-making during the flight.

MAVLink Protocol: To establish a secure and reliable communication link, the ground station leverages the MAVLink protocol. MAVLink is a lightweight communication protocol that has proven highly effective in the field of unmanned systems. It ensures that commands and data are transmitted between the ground station and the vehicle with precision and reliability.[10]

10. Communication System

The communication system serves as the fundamental bridge in the project.

10.1 Pixhawk- Raspberry Pi 4

The Raspberry Pi 4 Model B interacts with the flight controller through DroneKit. Additionally, the PX4 flight controller consistently transmits GPS and attitude data to the Raspberry Pi 4 Model B using the MAVLink protocol. These robust communication protocols ensure a reliable connection, enabling the transmission of critical data during flight.

The connection between the Raspberry Pi companion computer and Pixhawk is established using a wired, serial connection. The TELEM2 port of Pixhawk is connected to the RXD and TXD pins on the RPi. The VCC pin, which is used to provide power to the companion computer, is not utilized due to the Raspberry Pi receiving power from an external battery source. The simultaneous use of two power systems could potentially lead to voltage conflicts and irregularities, hence this situation has been addressed with caution. The baud rate is set to the default value of 921600 [16]

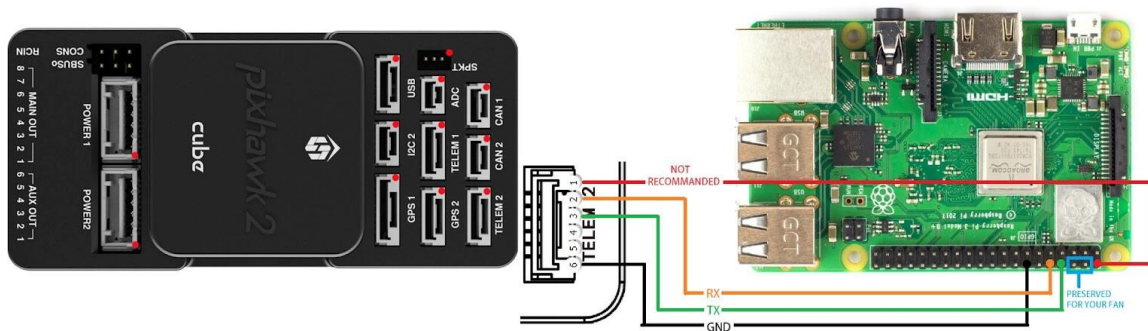


Image 13

Pin Connection of the Serial Protocol Communication

Communication between the Raspberry Pi and Pixhawk was established through DroneKit, which utilizes the MAVLink protocol. DroneKit is a robust software tool for communicating with and controlling a vehicle, known for its ease of use and development. This approach not only effectively fulfills the project's communication requirements but also takes advantage of the flexibility and customization options provided by the MAVLink protocol.

10.2 Ground Control Station and Communication

A HolyBro 433 MHz Telemetry Module is used for communication between the ground station and the vehicle. Since the TELEM1 port on PX4 is by default reserved for the ground station, the HolyBro module is also connected via the TELEM1 port, establishing a wired connection. The Baudrate for modules like GPS is automatically detected, and the default setting for manual operations is 57600 Baudrate.[17]